View metadata, citation and similar papers at core.ac.uk

brought to you by CORE

provided by Hiroshima University Institutional Repository

広島大学学術情報リポジトリ
Hiroshima University Institutional Repository

Title	Control of the incorporation and release of guest molecules by photodimerization in liposomes
Auther(s)	Shimokawa, Ryo; Ueda, Masafumi; Sugikawa, Kouta; Ikeda, Atsushi
Citation	Journal of Photochemistry and Photobiology B: Biology , 185 : 235 - 240
Issue Date	2018-08
DOI	10.1016/j.jphotobiol.2018.06.008
Self DOI	
URL	http://ir.lib.hiroshima-u.ac.jp/00046214
Right	Copyright (c) 2018 Elsevier B.V. This manuscript version is made available under the CC-BY-NC-ND 4.0 license. http://creativecommons.org/licenses/by-nc-nd/4.0/ This is not the published version. Please cite only the published version. この論文は出版社版でありません。引用の際には出版社版をご確認ご利用ください。
Relation	

Hiroshima University Institutional Repository

Graphical Abstract

To create your abstract, type over the instructions in the template box below.
Fonts or abstract dimensions should not be changed or altered.

Control of the incorporation and release of guest molecules by photodimerization in liposomes

Leave this area blank for abstract info.

Ryo Shimokawa, Masafumi Ueda, Kouta Sugikawa, and Atsushi Ikeda*

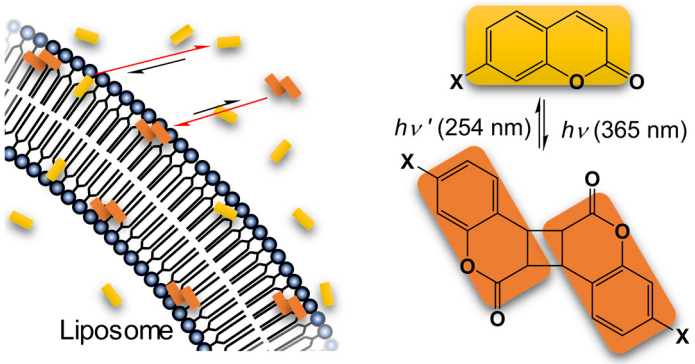

Control of the incorporation and release of guest molecules by photodimerization in liposomes

Ryo Shimokawa, Masafumi Ueda, Kouta Sugikawa, and Atsushi Ikeda*

Department of Applied Chemistry, Graduate School of Engineering, Hiroshima University, 1-4-1 Kagamiyama, Higashi-Hiroshima 739-8527, Japan

Keywords: Liposomes, Drug delivery, Photochemistry, Host-guest system, Dimerization

Abstract

In a drug-delivery system using liposomes, the use of guest molecules bearing hydrophilic moieties results in some leakage from lipid membranes. We suppressed the leakage of coumarins (used as model guest molecules in a drug-delivery system) from lipid membranes by photodimerization at 365 nm. The reason for this phenomenon could be ascribed to an increase in the hydrophobicity of the dimers of the coumarins. The formation of the dimers was detected by ^{1}H NMR, UV-vis absorption, and mass spectra and the leakage percentages of the coumarins were determined by ^{1}H NMR spectra based on the peak intensities. In contrast, when the dimer reverted to a monomer by ultraviolet (254 nm) irradiation, the resulting monomer was released from liposomes.

1. Introduction

In a drug-delivery system, it is very important to control the location of a drug, as well as the timing and amount of drug release in the target tissue (e.g., tumor) [1–5]. Heat, pH, light and enzymes can serve as triggers for controlled release. Liposomes have received increasing levels of attention because of their potential application as drug carriers because poorly water-soluble "guest molecules" (drugs) can be incorporated within lipid membranes [6]. Interest in liposomes as drug carriers is based on their potential to enclose various types of biologic/biomedical materials and to deliver them to diverse cell types [6]. Therefore, the stabilities of lipid membrane-incorporated guest molecules (LMIGs) are very important to increase their bioavailability and circulation in blood. However, the use of guest molecules bearing hydrophilic moieties could result in some leakage from lipid membranes or destabilization of LMIGs by the collapse of liposomes and micelle formation. Schwarzenbach et al. reported a method for determining the liposome–water distribution ratio (log K_{lipw}) of substituted phenols and several other compounds [7]. In contrast, we investigated the relationship between the equilibrium and octanol–water partition

coefficient (log P_{ow}) for some small model guest molecules with a π-moiety [8]. Our results showed that, in most of the guest molecules with log P_{ow} > 1.9, whole molecules were incorporated into liposomes to form stable LMIGs. However, many of the guest molecules with log P_{ow} < 1.9 leaked from the lipid membranes and dissolved in bulk water (Scheme 1a). That is, the threshold for leakage of guest molecules was determined to be ≈ 1.9. The log P_{ow} value of a guest molecule is usually defined as the ratio of its concentrations in the two phases of a mixture composed of 1-octanol and water [9]. The log P_{ow} values of guest molecules are usually determined experimentally. However, it is also possible to estimate these values using several commercially available computer programs [10]. Therefore, use of log P_{ow} values facilitates prediction of whether some guest molecules leak from lipid membranes. In the present study, we employed coumarins (**1** and **2**; Fig. 1) with relatively low log P_{ow} values (< 1.9) as small guest molecules, and controlled the incorporation and release of these molecules in liposomes by photodimerization (Scheme 1).

<Please insert Scheme 1>

<Please insert Fig. 1>

2. Materials and Methods

2.1. Materials

Coumarins **1** and **2** were purchased from Tokyo Chemical Industries (Tokyo, Japan). 1,2-Dimyristoyl-*sn*-glycero-3-phosphocholine (DMPC) was obtained from Funakoshi (Tokyo, Japan).

2.2. Preparation of liposomes

An appropriate amount of a mixture of DMPC and **1** or **2** ([DMPC]:[**1** or **2**] = 5:1 mol/mol) was dissolved in chloroform. The solvent was evaporated under a gentle stream of nitrogen, followed by a period under vacuum to remove trace solvent. The resulting thin lipid films were hydrated on the wall of the vial above the phase transition temperature with an appropriate amount of water. The hydrated materials were subjected to eight freeze–thaw cycles (–195 and +50 °C) to give unilamellar vesicles, which were extruded 11 times through 0.05-μm pores using a LiposoFast™ Mini-extruder (Avestin, Ottawa, ON, USA) above the phase transition temperature. The resulting liposomes were uniform in size with a diameter of ≈ 90 nm.

2.3. Determination of leakage percentages

The leakage percentages of **1** and **2** were determined using ^{1}H NMR spectra of LMI**1** and LMI**2** aqueous solutions (D_2O, [DMPC] = 4.0 mM, [DMPC]:[**1** or **2**] = 5:1 mol/mol). They were based on the peak intensities of **1** and **2** relative to the DMSO peak (0.4 mM), which was added as an internal reference.

2.4. Photoirradiation

Aqueous solutions of LMI**1** and LMI**2** (1.0 ml, [**1** or **2**] = 0.8 mM, [DMPC] = 4.0 mM) were photoirradiated at 365 nm for 12 h or 9 h, respectively, in a 1-cm quartz cell (1.0 W m^{-2}). Furthermore, these solutions were photoirradiated at 254 nm for 12 h and 4 h, respectively, in a 1-cm quartz cell (1.2 W m^{-2}). The photoreactions were monitored by UV-vis absorption and ^{1}H NMR spectra. The formation of dimer **1**-**1** was confirmed by GC-MS spectra and that of dimer **2**-**2** by GC-MS and ^{1}H NMR spectra.

*2.5. Separation of dimer **2-2***

An aqueous solution of LMI**2** (1.0 ml, [**2**] = 0.8 mM, [DMPC] = 4.0 mM) was photoirradiated at 365 nm for 9 h. The solution was lyophilized and the residue separated by preparative thin-layer chromatography on silica gel ($CHCl_3$, R_f = 0.05). The residue of the fraction was dissolved in $CDCl_3$ and was measured by ^{1}H NMR spectrum to determine containing dimer **2-2**.

2.6. UV-vis absorption spectra

UV-vis spectra were recorded using a UV-2550PC spectrophotometer (Shimadzu, Kyoto, Japan). All experiments were undertaken at 25 °C using a 1-mm cell.

2.7. ^{1}H NMR spectroscopy

^{1}H NMR data were recorded using a Varian 400-MR (400 MHz) spectrometer (Agilent Technologies, Santa Clara, CA, USA).

2.8. Gas chromatography–mass spectrometry (GC-MS)

The GC-MS system used was a JMS-T100GCV AccuTOF GCv 4G (JEOL, Tokoyo, Japan) equipped with a 30 m × 0.25 mm I.D. fused-silica capillary column (J&W; HP-5; film thickness, 0.25 μm). The column temperature was set at 50 °C for 1 min, and then it was programmed to heat from 50 °C to 300 °C at 10 °C/min. The temperature of the injection port and interface was set at 300 °C. Splitless injection mode was used. Helium at a flow rate of 1.5 ml/min was used as a carrier gas. Target analytes underwent chemical ionization at 200 eV and were detected in scan mode. Target ions had a *m*/*z* of 293 for dimer **1**-**1** and 353 for dimer **2**-**2** as $[M+H]^+$, respectively.

3. Results and Discussion

3.1. Formation of LMIGs by the premixing method

Liposomes consisting of dimyristoylphosphatidylcholine (DMPC) were prepared in the presence of coumarin (**1**) or 7-methoxycoumarin (**2**) according to the premixing method [6,8,11–14]. Briefly, LMI**1**

and LMI**2** were prepared by dissolving DMPC and **1** or **2** in chloroform, followed by evaporation of chloroform under a stream of dry nitrogen gas to give a residue. Multilamellar vesicles (MLVs) were prepared by hydration of the dried lipid films by vortexing. To change from multilamellar to unilamellar vesicles and to obtain a narrow size distribution, the solution was repeatedly frozen and thawed eight times and extruded eleven times with two stacked polycarbonate membranes with a pore size of 50 nm.

The UV-vis absorption spectra of LMI**1** and LMI**2** showed that **1** and **2** were dissolved in water (Fig. 2a, b; black line). However, the results did not indicate whether all of **1** and **2** were incorporated in lipid membranes because hydrophilic **1** and **2** might have leaked from lipid membranes [8].

<Please insert Fig. 2>

*3.2. Leakage percentages of monomer **1** and dimer **1-1** from liposomes*

We have reported that the proton nuclear magnetic resonance (^{1}H NMR) spectrum of LMI**1** contains several peaks in the range 6.4–8.2 ppm (Figs. 3 and S1) [8]. Because peaks belonging to the guest molecules and lipids in LMIGs should have mostly disappeared due to peak broadening, these peaks were assignable to **1** having leaked from lipid membranes to bulk water (Figs. 3a and S1a) [8]. The leakage percentage of **1** was determined to be 65% for [**1**]/[DMPC] = 20.0 mol% based on the peak intensities of compound **1** relative to DMSO (0.4 mM), which was added as an internal reference (Table 1). The leakage percentage of **1** was scarcely affected by the concentration of **1** ([**1**]/[DMPC] = 5.0–20.0 mol%, Table 1 and Fig. S2). It is well-known that **1** photodimerizes under irradiation at 365 nm to give four regioisomers and stereo-isomers (Scheme 2) [15]. Therefore, we carried out the photodimerization of **1** in a mixture of **1** and liposomes. After photoirradiation at 365 nm for 12 h, the absorption peak at ≈ 275 nm decreased (Fig. 2a, red line). This result suggested that the formation of dimer **1-1** (Scheme 2) shortened a π-conjugation length by changing from a double bond of **1** to the cyclobutane of dimer **1-1**. The latter was detected at a mass-to-charge ratio (*m*/*z*) of 293.1 during gas chromatography–mass spectrometry (GC-MS) (Fig. 4). After photodimerization, the leakage percentage of **1** decreased from 65% to 28% as determined by the peak intensities in the ^{1}H NMR spectrum (Table 1). Although the solution was exposed to light at 365 nm for a much longer time, the leakage percentage scarcely changed and the absorbance of monomer **1** remained, which may have been due to the low yield of the photodimerization. No peaks assigned to dimer **1-1** were observed in the ^{1}H NMR spectrum (Figs. 3b and S1b), indicating that dimer **1-1** was incorporated within liposomes. We wanted to ascertain why dimer **1-1** was incorporated into lipid membranes. We have reported that whole molecules are incorporated into liposomes in most guest molecules with log P_{ow} > 1.9. Although the log P_{ow} value of **1** is 1.39 [10], that of dimer **1-1** can be calculated to be 3.22 and 3.14 for head-to-head and head-to-tail isomers, respectively. A large value in log P_{ow} denotes high hydrophobicity, so an increase of hydrophobicity led to complete incorporation of dimer **1-1** into liposomal membranes.

<Please insert Fig. 3>

<Please insert Fig. 4>

<Please insert Table 1>

<Please insert Scheme 2>

*3.3. Photoreactions from dimer **1-1** to monomer **1***

We attempted to breakdown dimer **1**-**1** into monomer **1** by photoirradiation at 254 nm for 12 h. However, because the UV-vis absorption and ^{1}H NMR spectra scarcely changed after photoirradiation (Fig. 2a, blue line; Fig. 3c; Fig. S1c), the photoreaction barely proceeded. The leakage percentage decreased from 28% to 18%. Although monomer **1**, having leaked from lipid membranes reacts by photoirradiation at 254 nm, monomer **1** was not decomposed by photoirradiation at 254 nm in the absence of liposomes (Fig. S3). Therefore, we suggest two possible explanations for this decrease: (i) after photoirradiation at 365 nm, dimer **1**-**1** inhibited the incorporation of monomer **1** in liposomes because dimer **1**-**1**, with its polar groups was expected to locate near the liposomal surface, or (ii) after the photoirradiation at 254 nm, the by-products decomposed from dimer **1**-**1** supported the incorporation of monomer **1** in liposomes because the by-products interact with monomer **1** in lipid membranes. However, because by-products have not yet been revealed, the reasons for the decrease in the amount of monomer **1** are not clear at present.

*3.4. Leakage percentages of monomer **2** and dimer **2-2** from liposomes*

Under a solid condition, the photodimerization of **2** gives a higher yield than that of **1** [16]. Therefore, we employed **2** as a guest molecule in liposomes. Although the log P_{ow} value of **2** (1.78) was higher than that of **1** (1.39), the leakage percentage of **2** (71%) was higher than that of **1** (65%) ([DMPC] = 4.0 mM, [**1** or **2**]/[DMPC] = 20 mol%) (Table 1; Figs. 3d and S4a). Log P_{ow} values are not required to ascertain the leakage percentage [8].

After photoirradiation at 365 nm for 9 h, most of **2** gave dimer **2**-**2** as suggested by the UV-vis absorption spectrum in which the absorbance of **2** decreased (Fig. 2b, red line). The leakage percentage of **2** decreased from 71% to < 2%, indicating that almost all of **2** was incorporated in liposomes. Because no peak assigned to dimer **2**-**2** was observed in the ^{1}H NMR spectrum (Figs. 3e and S4b), most of dimer **2**-**2** was incorporated in liposomes. The reason could also be ascribed to an increase in log P_{ow} by dimerization (3.27 and 3.19 for head-to-head and head-to-tail isomers, respectively). To confirm the formation of dimer **2**-**2**, we observed GC-MS spectra (Fig. 5). Dimer **2**-**2** was detected at *m*/*z* 353.1 (Fig. 5b). For further confirmation, the solution after photoirradiation was lyophilised and the residue separated by preparative thin-layer chromatography on silica gel ($CHCl_3$, retardation factor (R_f) = 0.05). In the ^{1}H NMR spectrum of the fraction (Figs. 6 and S5), several peaks appeared at similar positions to the chemical shifts of the

peaks assigned to dimer **2**-**2** as a *syn*-head-to-tail isomer (Scheme 2) in a report by Gnanaguru *et al*. [16] After photoirradiation at 254 nm, about half of dimer **2**-**2** reverted to monomer **2** (Fig. 2b, blue line). The reason for this ≈ 50% yield may be that a cyclobutane ring of **2** was cleaved at other positions in a similar way [17]. Consequently the leakage percentage of **2** increased to 22%. The UV-vis absorption spectrum did not change upon further photoirradiation for 4 h. A similar experiment was undertaken under a nitrogen atmosphere to ascertain if there had been interference by oxygen. A similar result was obtained (Fig. 2c), showing that oxygen did not influence the reaction (Table 1).

<Please insert Fig. 5>

<Please insert Fig. 6>

3.5. Photodimerization rates in the absence and presence of liposomes

To ascertain if the photodimerization of **1** occurred inside or outside liposomal membranes, we measured the photodimerization rate of **1** based on changes in the UV-vis absorption spectra at 278 nm and 276 nm in the absence and presence of liposomes, respectively (Fig. 7). The calculated rate constants (in M^{-1} s^{-1}) of **1** were k = 96 (r = 0.989) and 52 (r = 0.977) in the presence and absence of liposomes, respectively. The photodimerization rate in liposomes was approximately two-times faster than that in the absence of liposomes. However, acceleration of the photodimerization rate by liposomes was slight compared with the photodimerization of anthracene in liposomes [18]. Even considering the low abundance of **1** in liposomal membranes (35%, Table 1), the photodimerization rate in liposomes was estimated to be k = 275 M^{-1} s^{-1} and was about five-times faster than that in the absence of liposomes. The photodimerization rate was not fast enough for most of **1** to react within liposomes. The photodimerization of **2** based on changes in the UV-vis absorption spectra at 322 nm and 324 nm in the absence and presence of liposomes, respectively, is shown in Fig. 8. The calculated rate constants (in M^{-1} s^{-1}) of **2** were k = 1290 (r = 0.987) and 1100 (r = 0.991) in the presence and absence of liposomes, respectively (Fig. 8). The photodimerization rate in liposomes was estimated to be k = 4450 M^{-1} s^{-1} using an abundance of **2** in liposomal membranes (29%, Table 1). The rate was about fourfold faster than that in the absence of liposomes. Consequently, the photodimerization of **1** and **2** did not exhibit a concentration effect by liposomes because of the low abundance of **1** and **2** in liposomal membranes. These results suggest that the photodimerization of **1** and **2** occurred inside and outside liposomal membranes. A precipitate was not observed after photodimerization, so most of dimers **1**-**1** and **2**-**2** outside liposomal membranes were incorporated within liposomes.

<Please insert Fig. 7>

<Please insert Fig. 8>

3.6. Change of liposome size by photodimerization

The size distributions of liposomes were studied using dynamic light scattering (DLS). Table 2 shows that the D_{hy} (in nm) changed from 92 and 87 before photodimerization to 97 and 80 after photodimerization for LMI**1** and LMI**2**, respectively. This finding suggested that incorporation of dimer **1**-**1** and **2**-**2** had very little impact on liposome size.

<Please insert Table 2>

4. Conclusion

In summary, most of the coumarins **1** and **2** leaked from hydrophobic liposomal membranes because of their hydrophilicity. Their leakage was prevented by photodimerization because of increasing their hydrophobicity. Photodimerization of **1** was not complete, and **1** remained as a monomer outside liposomes. Furthermore, dimer **1**-**1** did not revert to a monomer **1** by photoirradiation at 254 nm. In contrast, **2** was incorporated completely in liposomes by photodimerization. Furthermore, dimer **2**-**2** reverted to a monomer **2** by photoirradiation at 254 nm, and part of the monomer was released from liposomal membranes. Control of the incorporation and release of guest molecules is dependent upon the log P_{ow} values between monomers and dimers.

Acknowledgments

This work was supported by a JSPS KAKENHI Grant-in-Aid for Scientific Research (B) (Grant No. JP16H04133) and a Grant-in-Aid for Challenging Exploratory Research (Grant No. JP16K13982). We thank the Edanz Group (www.edanzediting.com/ac) for editing a draft of this manuscript.

References

[1] A.D. Bangham, Membrane models with phospholipids, Prog. Biophys. Mol. Biol. 18 (1968) 29–36.

[2] G. Sessa, G. Weissmann, Phospholipid spherules (liposomes) as a model for biological membranes, J. Lipid Res. 9 (3) (1968) 310–318.

[3] Y. Kaneda, Virosomes: evolution of the liposome as a targeted drug delivery system, Adv. Drug Delivery Rev. 43 (2–3) (2000) 197–205.

[4] T.M. Allen, P.R. Cullis, Drug delivery systems: Entering the mainstream, Science 303 (5665) (2004) 1818–1822.

[5] V.P. Torchilin, Recent advances with liposomes as pharmaceutical carriers, Nat. Rev. Drug Discovery 4 (2) (2005) 145–160.

[6] Liposomes: A Practical Approach (Eds.: V. P. Torchilin, W. Weissig), 2nd ed., Oxford University Press, Oxford (UK), 2003.

[7] B.I. Escher, R.P. Schwarzenbach, Partitioning of substituted phenols in liposome-water, biomembrane-water, and octanol-water systems, Environ. Sci. Technol. 30 (1) (1996) 260–270.

[8] A. Ikeda, K. Ashizawa, Y. Tsuchiya, M. Ueda, K. Sugikawa, Formation of lipid membrane-incorporated small π-molecules bearing hydrophilic groups, RSC Adv. 6 (82) (2016) 78505–78513.

[9] Y. Katz, J.M. Diamond, A method for measuring nonelectrolyte partition coefficients between liposomes and water, J. Membrane Biol. 17 (1) (1974) 69–86.

[10] The values of log Pow were calculated using Advaced Chemistry Development Software V11.02 (ACD/labs.).

[11] A.D. Bangham, M.M. Standish, J.C. Watkins, Diffusion of univalent ions across the lamellae of swollen phospholipids, J. Mol. Biol. 13 (1) (1965) 238–252.

[12] A. Ikeda, T. Hida, T. Nakano, S. Hino, K. Nobusawa, M. Akiyama, K. Sugikawa, Stability of lipid-membrane-incorporated azobenzene and pyrenes in water, Chem. Lett. 43 (10) (2014) 1551−1553.

[13] A. Ikeda, S. Hino, K. Ashizawa, K. Sugikawa, J. Kikuchi, M. Tsukamoto, K. Yasuhara, Lipid-membrane-incorporated hydrophobic photochromic molecules prepared by the exchange method using cyclodextrins, Org. Biomol. Chem. 13 (22) (2015) 6175–6182.

[14] M. Ueda, K. Ashizawa, K. Sugikawa, K. Koumoto, T. Nagasaki, A. Ikeda, Lipid-membrane-incorporated arylboronate esters as agents for boron neutron capture therapy, Org. Biomol. Chem. 15 (7) (2017) 1565−1569.

[15] K. Muthuramu, V. Ramamurthy, Photodimerization of coumarin in aqueous and micellar media, J. Org. Chem. 47, (20) (1982) 3976−3979.

[16] K. Gnanaguru, N. Ramasubbu, K. Venkatesan, V. Ramamurthy, A study on the photochemical dimerization of coumarins in the solid state, J. Org. Chem. 50 (13) (1985) 2337−2346.

[17] T. Wolff, H. Görner, Photocleavage of dimers of coumarin and 6-alkylcoumarins, J. Photochem. Photobiol., A 209 (2–3) (2010) 219–223.

[18] Y. Tsuchiya, K. Sugikawa, M. Ueda, A. Ikeda, Incorporation of large guest molecules in liposomes via chemical reactions in lipid membranes, Org. Biomol. Chem. 15 (8) (2017) 1786–1791.

Table 1. Leakage percentages of coumarins before and after photoirradiation {D_2O, [DMPC] = 4.0 mM, [**1**]/[DMPC] = 5–20 mol%, [**2**]/[DMPC] = 20 mol%, [DMSO] = 0.4 mM (internal reference for peak intensity)}.

Guest molecule	[G]/[DMPC] (mol%)	Conditions	Leakage percentage (%)		
			Before	365 nm	254 nm
1	5	Air	70[a]	34[b]	6[d]
1	10	Air	75[a]	31[b]	17[d]
1	20	Air	65[a]	28[b]	18[d]
2	20	Air	71[a]	< 2[c]	22[c]
2	20	N_2	64[a]	< 2[c]	14[c]

[a] Before photoirradiation.

[b] After photoirradiation at 365 nm for 12 h.

[c] After photoirradiation at 365 nm for 9 h.

[d] After photoirradiation at 254 nm for 12 h.

[e] After photoirradiation at 254 nm for 4 h.

Table 2. Average hydrodynamic diameters D_{hy} (nm), as determined using a light-scattering method at 25 °C before and after photoirradiation.

	Before		365 nm		254 nm	
	D_{hy} (nm)	PDI[a]	D_{hy} (nm)	PDI[a]	D_{hy} (nm)	PDI[a]
LMI**1**	92	0.084	97	0.059	92	0.097
LMI**2**	87	0.037	80	0.067	77	0.093

[a] PDI: Polydispersity index.

Scheme captions

Scheme 1. Guest molecules (yellow) and guest dimers (orange) before (a) and after photoirradiation at 365 nm (b) and 254 nm (c) inside and outside the lipid membrane (schematic).

Scheme 2. Photodimerization of coumarins and their log P_{ow} values.

Figure captions

Fig. 1. Structures of compounds.

Fig. 2. UV-vis absorption spectra of (a) LMI**1** and (b) LMI**2** under an air atmosphere and (c) LMI**2** under a nitrogen atmosphere before photoirradiation (black line), after photoirradiation at 365 nm (a) for 12 h or (b and c) for 9 h (red line), and after photoirradiation at 254 nm for (a) 12 h or (b and c) for 4 h (blue line)

Fig. 3. Partial ^{1}H NMR spectra of LMI**1** (a) before photoirradiation, (b) after photoirradiation at 365 nm for 12 h and then (c) after photoirradiation at 254 nm for 12 h. Partial ^{1}H NMR spectra of LMI**2** (d) before photoirradiation, (e) after photoirradiation at 365 nm for 9 h and then (f) after photoirradiation at 254 nm for 4 h {D_2O, [DMPC] = 4.0 mM, [**1** or **2**]/[DMPC] = 20 mol%, [DMSO] = 0.4 mM (internal reference for peak intensity)}.

Fig. 4. (a) GC-MS chromatogram of LMI**1** obtained after photoirradiation at 365 nm for 12 h and (b) MS spectrum of the retention time at 21.76–21.77 min in the chemical ionization mode.

Fig. 5. (a) GC-MS chromatogram of LMI**2** obtained after photoirradiation at 365 nm for 9 h and (b) MS spectrum of the retention time at 24.94–24.95 min in the chemical ionization mode.

Fig. 6. Partial ^{1}H NMR spectrum of dimer **2-2** separated from a LMI**2** solution by column chromatography (silica gel, $CHCl_3$) after photoirradiation at 365 nm for 9 h (●: *syn*-head-to-tail isomer, $CDCl_3$).

Fig. 7. UV-vis absorption spectra of **1** (a) in the absence and (b) in the presence of liposomes in water at 25 °C for irradiation times 0, 1, 2, 3, 4, 5, 6, 7, 8, and 9 h ([**1**] = 0.8 mM, [DMPC] = 0 or 4.0 mM). Inset: plot of $1/[\mathbf{1}] - 1/[\mathbf{1}]_0$ versus irradiation time.

Fig. 8. UV-vis absorption spectra of **2** (a) in the absence and (b) presence of liposomes in water at 25 °C for irradiation times 0, 0.5, 1.0, 1.5, 2.0, 2.5, and 3.0 h ([**2**] = 0.8 mM, [DMPC] = 0 or 4.0 mM). Inset: plot of $1/[\mathbf{2}] - 1/[\mathbf{2}]_0$ versus irradiation time.

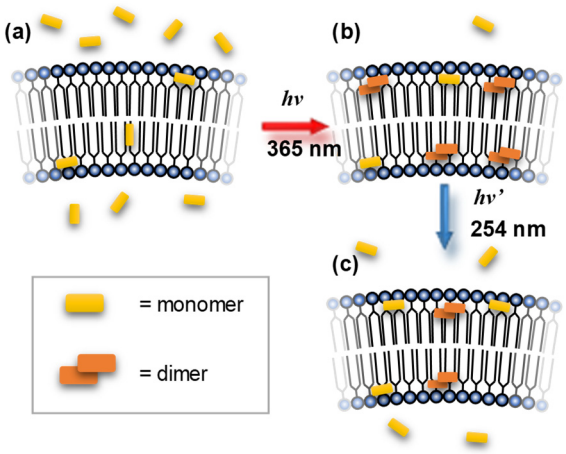

Scheme 1

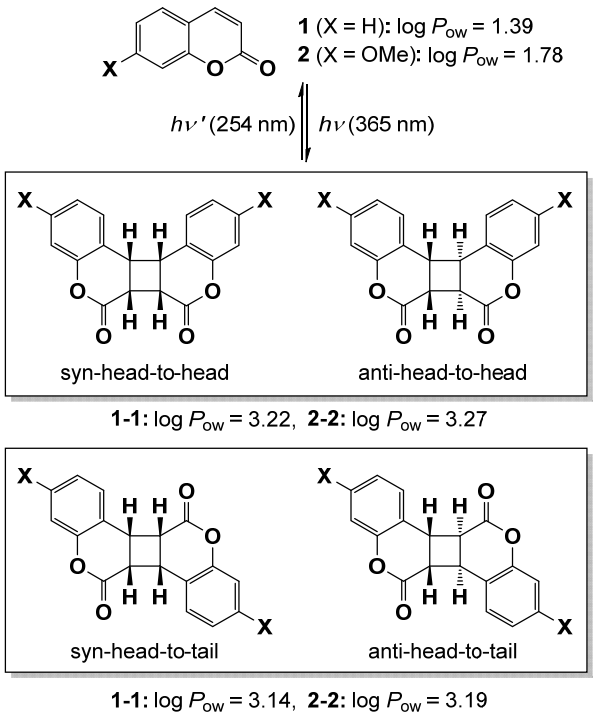
1 (X = H): log P_{ow} = 1.39
2 (X = OMe): log P_{ow} = 1.78
hν′(254 nm)
hν(365 nm)
syn-head-to-head
anti-head-to-head
1-1: log P_{ow} = 3.22, 2-2: log P_{ow} = 3.27
syn-head-to-tail
anti-head-to-tail
1-1: log P_{ow} = 3.14, 2-2: log P_{ow} = 3.19

Scheme 2

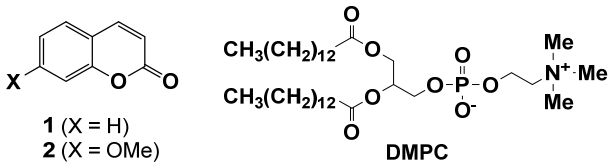

Fig. 1

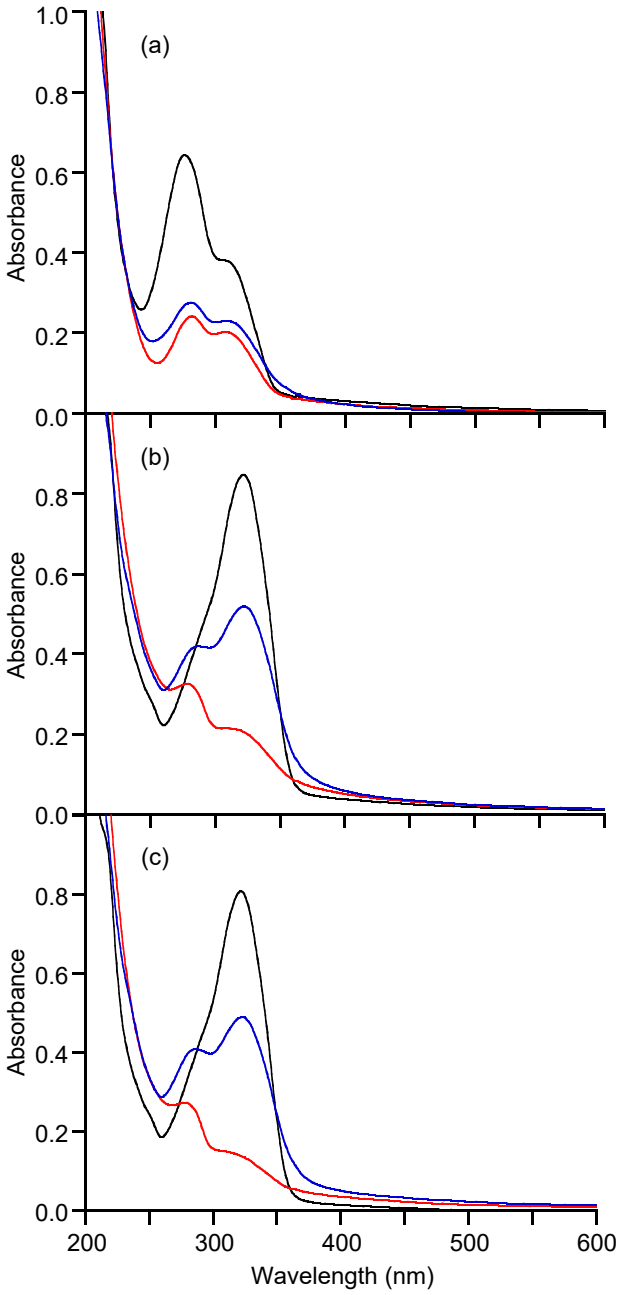
(a)
(b)
(c)
Absorbance
Absorbance
Absorbance
1.0
0.8
0.6
0.4
0.2
0.0
200
300
400
500
600
Wavelength (nm)

Fig. 2

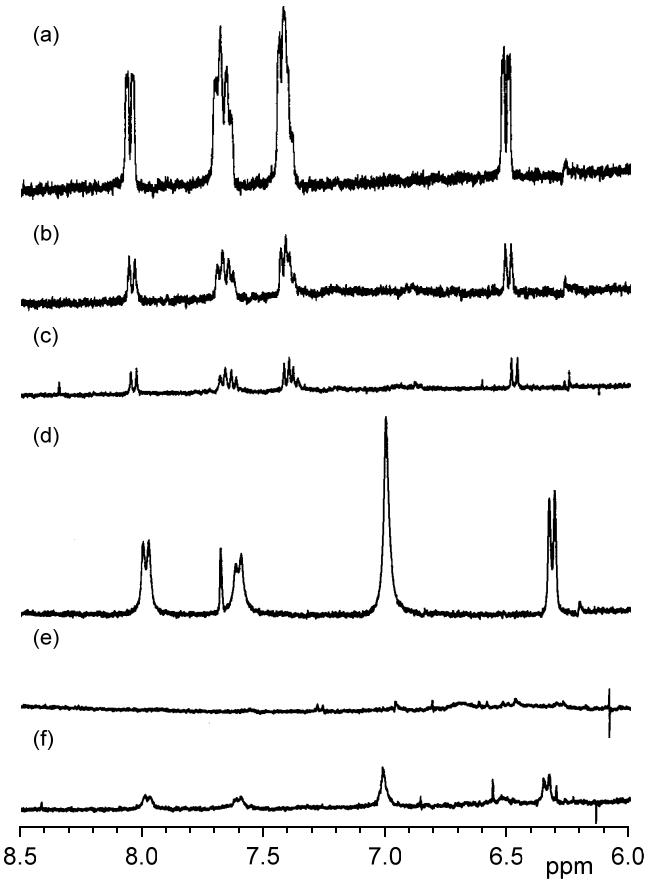

Fig. 3

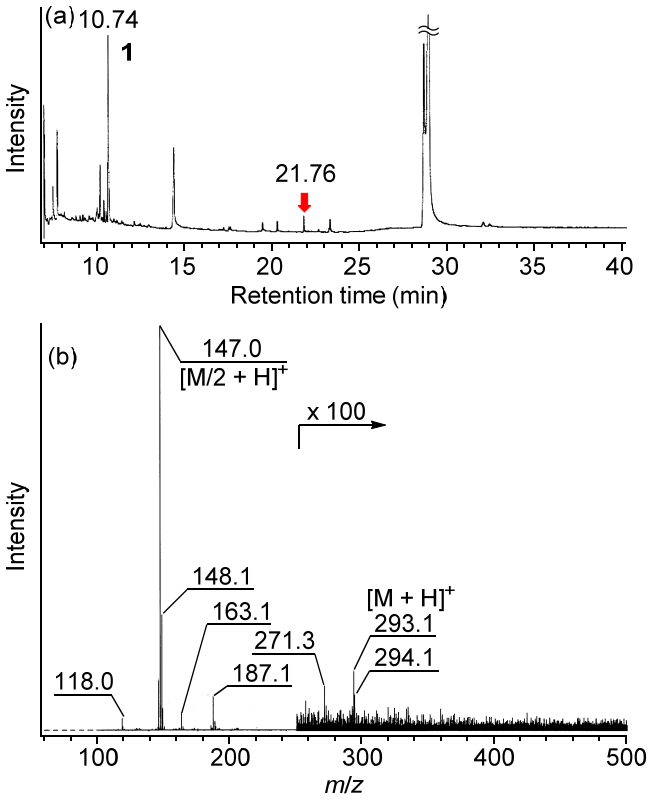
(a)
10.74
1
21.76
Intensity
10
15
20
25
30
35
40
Retention time (min)
(b)
147.0
[M/2 + H]+
x 100
148.1
163.1
271.3
187.1
118.0
[M + H]+
293.1
294.1
Intensity
100
200
300
400
500
m/z

Fig. 4

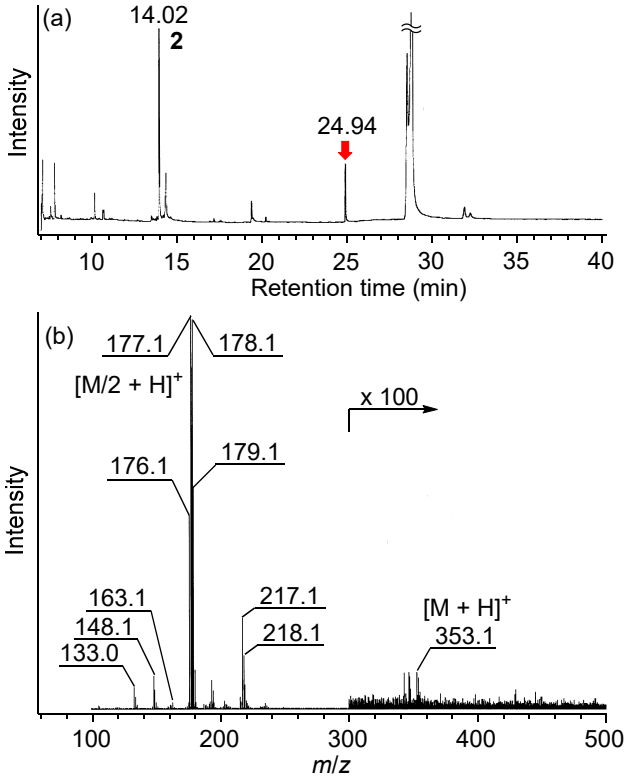
(a)
14.02
2
24.94
Intensity
10
15
20
25
30
35
40
Retention time (min)
(b)
177.1
178.1
[M/2 + H]+
x 100
176.1
179.1
Intensity
163.1
148.1
133.0
217.1
218.1
[M + H]+
353.1
100
200
300
400
500
m/z

Fig. 5

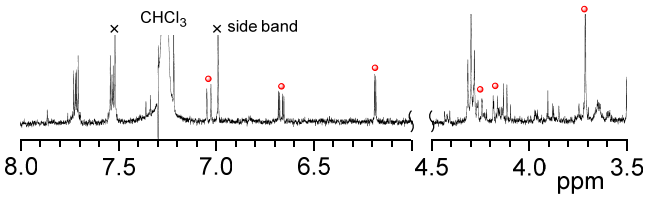

Fig. 6

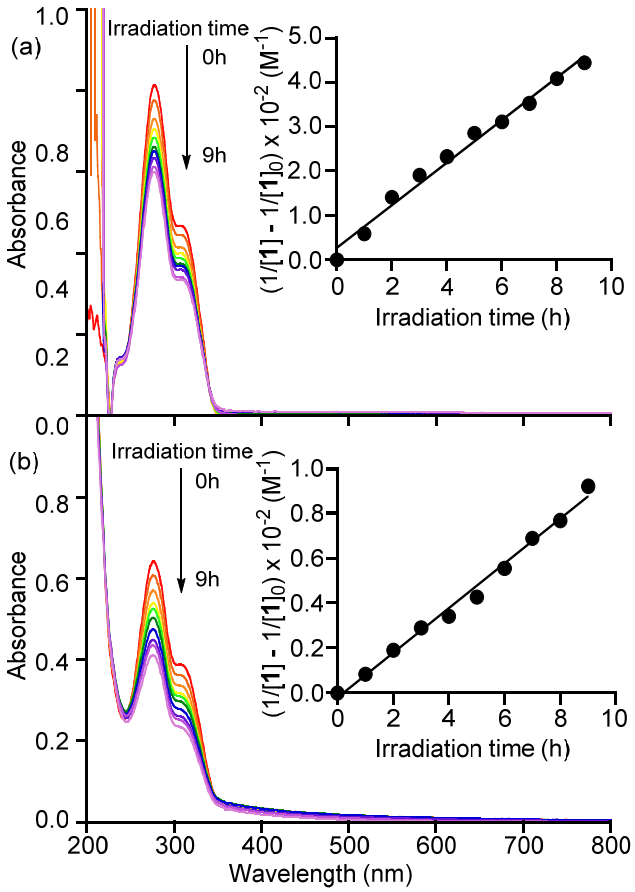
(a)
Irradiation time
0h
9h
Absorbance
1.0
0.8
0.6
0.4
0.2
0.0
(1/[1] - 1/[1]0) x 10-2 (M-1)
5.0
4.0
3.0
2.0
1.0
0.0
0
2
4
6
8
10
Irradiation time (h)
(b)
Irradiation time
0h
9h
Absorbance
1.0
0.8
0.6
0.4
0.2
0.0
(1/[1] - 1/[1]0) x 10-2 (M-1)
1.0
0.8
0.6
0.4
0.2
0.0
0
2
4
6
8
10
Irradiation time (h)
200
300
400
500
600
700
800
Wavelength (nm)

Fig. 7

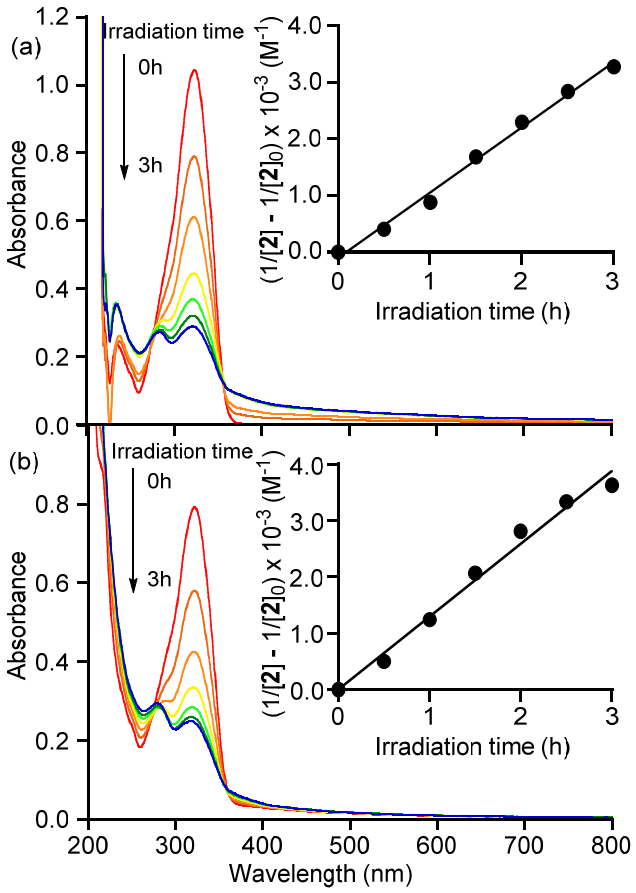
(a)
Irradiation time
0h
3h
Absorbance
1.2
1.0
0.8
0.6
0.4
0.2
0.0
(1/[2] - 1/[2]0) x 10-3 (M-1)
4.0
3.0
2.0
1.0
0.0
0
1
2
3
Irradiation time (h)
(b)
Irradiation time
0h
3h
Absorbance
1.2
1.0
0.8
0.6
0.4
0.2
0.0
(1/[2] - 1/[2]0) x 10-3 (M-1)
4.0
3.0
2.0
1.0
0.0
0
1
2
3
Irradiation time (h)
200
300
400
500
600
700
800
Wavelength (nm)

Fig. 8